

I Motivation

The Indian Summer Monsoon (ISM) presents a biennial and a decadal component. The issues addressed in this poster are:
Do the QBO (Quasi-Biennial Oscillation) and the 11-year solar cycle modulate the Indian summer monsoon, and what are the involved mechanisms?

II. Data and Method

NCEP-R2 reanalysis (1979-2001)
Winds at 850 and 200 hPa from NCEP-R2 have been considered to characterize the monsoon surface and upper-level circulation, respectively. The 500 hPa vertical velocity (w) has also been considered to describe the areas of deep convection.

Independent observational datasets
- **Precipitation**: global CMAP (Climate Prediction Center Merged Analysis Precipitation, Xie and Arkin (1997) precipitation fields and the All India Rainfall Index, Parthasarathy (1995) for an Indian Monsoon Rainfall (IMR) index.
- **Sea Surface Temperature (SST)**: Extended Reconstructed SST (ERSST), which correspond to a monthly extended reconstruction of global SST based on Comprehensive Ocean-Atmosphere Data Set (Smith and Reynolds, 2004). Available after 1854 on a 2° spatial grid at: <http://11w.f.ncei.noaa.gov/oa/climate/research/sst/sst.html#ersst>.
- **Mean sea level pressures (mslp)**: from the Hadley Centre, available since 1850 (5° latitude by 5° longitude).
- **QBO Index**: Mean equatorial zonal winds for levels between 70 and 10 hPa, from the Free University of Berlin (Naujokat, 1986; <http://strat-www.met.fu-berlin.de>) from 1953 on (1956 for the 10 hPa level).
- **Solar Index**: 10.7-cm radio flux (F10.7), which closely tracks the temporal behaviour of the Ultra-Violet changes on 11-yr time scales. Since it is not available before 1956, the sunspot number, which spans the longest time period, has been considered for the analysis of mslp and ERSST. It is available at: <http://sdc.oma.be/>.

Statistical analysis
To highlight the space-time structure of the monsoon and the QBO (solar) -monsoon links, standard lead-lag cross-correlation and regression techniques between mean equatorial zonal winds (F10.7 or the sunspot number for longer time series) and atmospheric fields are performed at each grid point. Volcanic effects are accounted for by considering the Atmospheric Optical Thickness provided on <http://data.giss.nasa.gov/modeler/force/stratrea> extended to 2001 by keeping the 1999 level constant. Finally, previous studies on the ISM-ENSO relationship have shown that a majority of warm episodes in the central and eastern equatorial Pacific are accompanied by below-normal summer rainfall over India. For this reason, the ENSO signal is also removed from the original time series by the linear regression method.
The statistical significance of the results is assessed with a phase-scrambling bootstrap test with 999 samples (Davison and Hinkley, 1997), taking into account the autocorrelation characteristics of the time series.

III Monsoon characteristics

At 850 hPa, the prominent monsoon wind systems are first the cross-equatorial flow along the east coast of Africa (see Figure 1a which provides a northern summer climatology of the wind at 850 hPa and omega at 500 hPa) and second the easterly trade winds in the tropical Pacific. Under the effect of the Coriolis force, the cross equatorial flow becomes the southwest monsoon in South Asia and meets with the trade winds in the western Pacific. Two rainfall maxima are observed over India and the surrounding Indian Ocean during the monsoon season (Figure 1b): one over the Bay of Bengal which extends northwestward into eastern and central India, and one along the western coast of India.

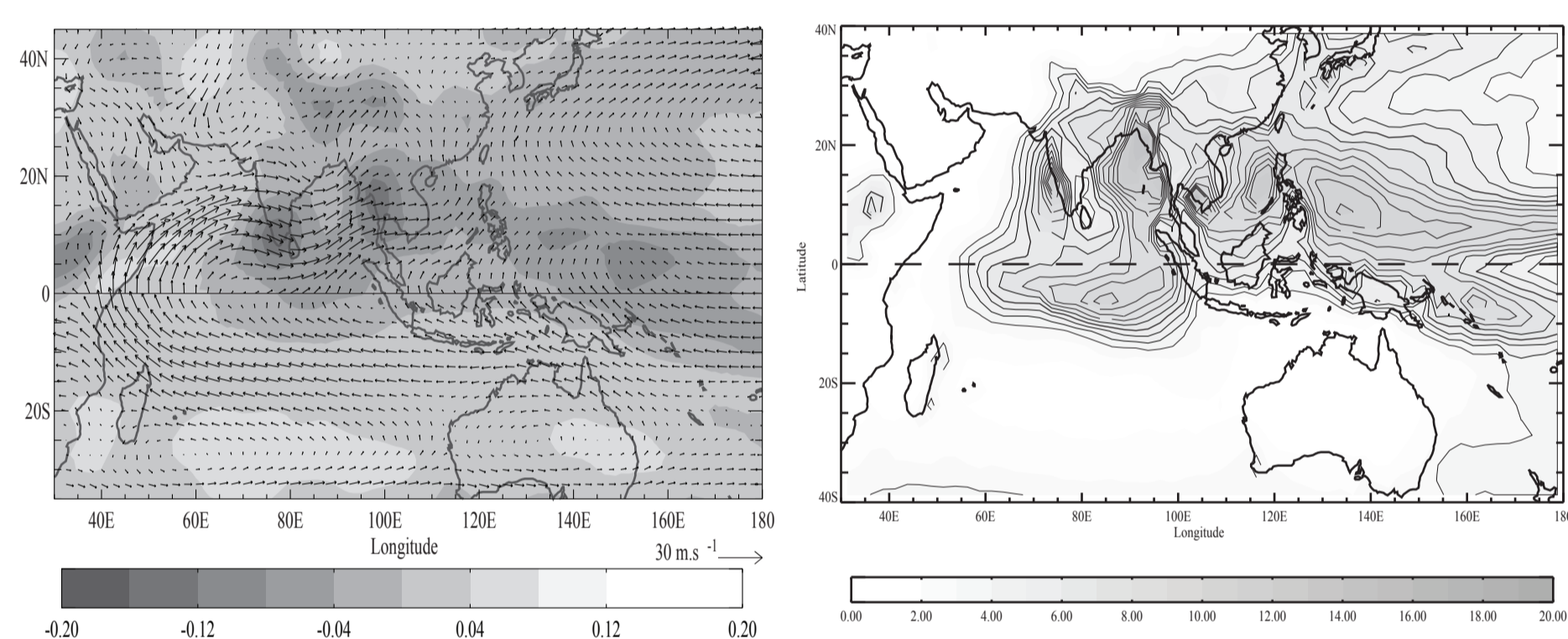


Figure 1a) 850 hPa wind (m/s) and 500 hPa vertical velocity (Pa/s) (June to September) climatology from CMAP (1979-2001).

IV. Indian Monsoon Rainfall / tropospheric circulation

At the surface, larger precipitation is associated with an enhancement of the monsoon low-level gyre circulation is observed during both the early (e.g. July) and late (e.g. September) ISM. The most significant surface and upper-level circulation anomalies with respect to the cumulated seasonal rainfall for India as a whole occur during September: large and significant negative 500 hPa vertical velocity anomalies are observed along the axis of the monsoon trough in the Gangetic plains. Broad-scale and significant anomalous circulation patterns with a westward shift of the Mascarene High are also observed in the South Indian Ocean.

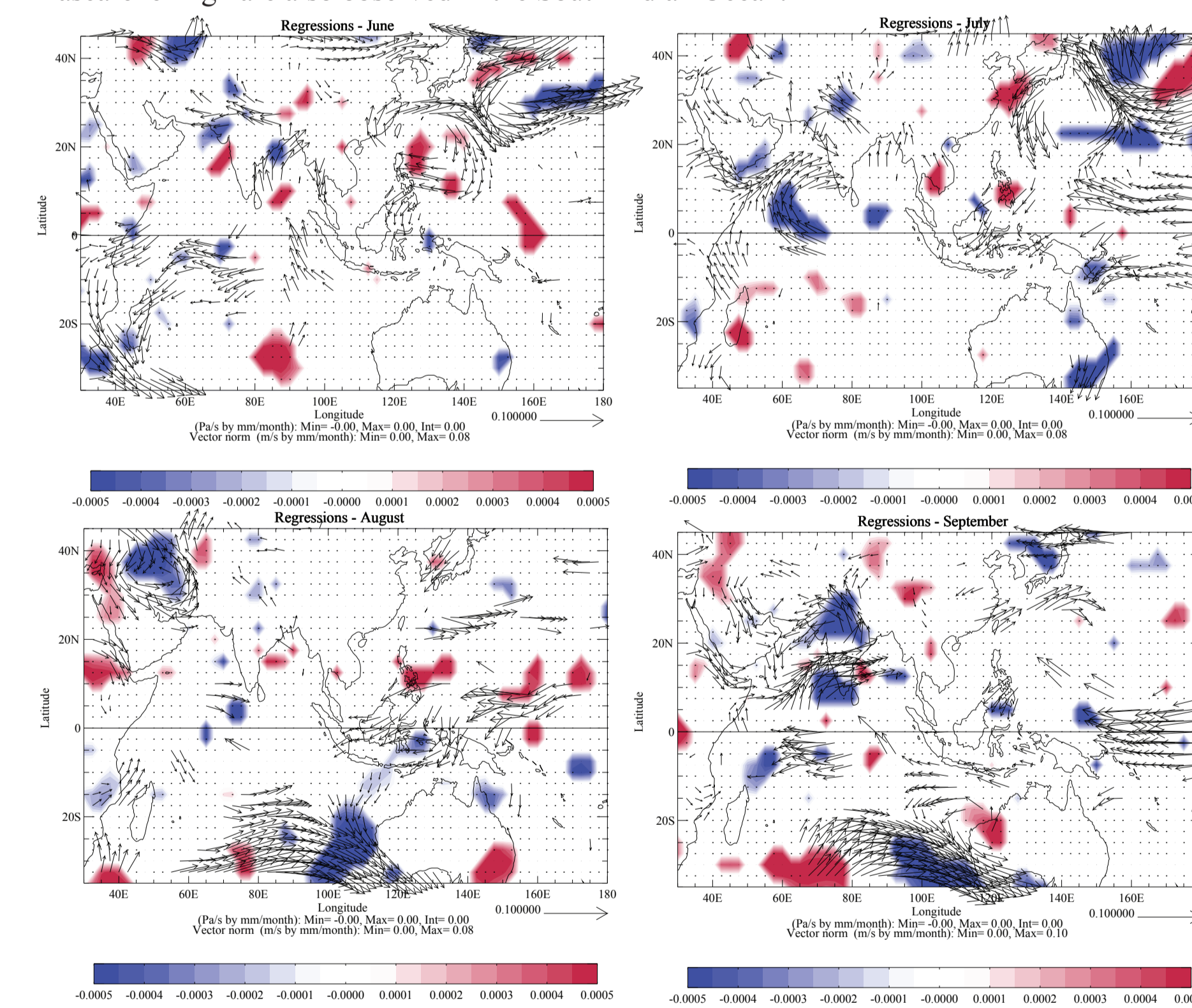


Figure 2. Distribution of monthly regression coefficients of NCEP-R2 850 hPa wind and 500 hPa vertical velocity versus IMR (June to September). Maps only show wind vectors and omega values corresponding to regression coefficients above the 90% confidence level.

REFERENCES

Baldwin, M. P., L. J. Gray, K. Hamilton, P. H. Haynes, W. J. Randel, J. R. Holton, M. J. Alexander, I. Hirota, T. Horinouchi, D. B. A. Jones, J. S. Kinnerson, C. Marquardt, K. Sato, and M. Takahashi (2001), *The Quasi-biennial oscillation*. Rev. Geophys., **39**, 2, 179-229.
Davison, A.C., and D.V. Hinkley (1997), *Bootstrap Methods and their Application*, Cambridge University Press, 582 pp.
Kodera, K. (2004), *Solar influence on the Indian Ocean Monsoon through dynamical processes*, Geophys. Res. Lett., **31**, L24209.
Naujokat, B., (1986), *An update of the observed Quasi-Biennial Oscillation of the stratospheric winds over the tropics*. J. Atmos. Sci., **43**, 1873-1877.
Parthasarathy, B., A.A. Munot, and D.R. Kothavale (1995), *All India monthly and seasonal rainfall series: 1871-1993*. Theor. Appl. Climatol., **49**, 217-224.
Smith T.S., and R.W. Reynolds (2004), *Improved Extended Reconstruction of SST (1854-1997)*, J. Clim., **17**, 2466-2477.
Terray, P., P. Delecluse, S. Labattu, and L. Terray (2003), *Sea Surface temperature associations with the late summer monsoon*. Clim. Dyn., **21**, 593-618.
Xie, P., and P.A. Arkin (1997), *Global Precipitation: A 17-Year Monthly Analysis Based on Gauge Observations, Satellite Estimates and Numerical Model Outputs*. Bull. Am. Meteorol. Soc., **78**, 2539-2558.

Acknowledgments

This work was partly supported by the French ANR STT-CLIM (Stratosphere impact on Tropical climate). The NCEP-R2 reanalyses and CMAP datasets were provided by the NOAA Climate Center (<http://www.cdc.noaa.gov>) through ClimServ (IPSL).

V. QBO/ Monsoon

The largest correlations between the QBO and IMR, reaching 0.38, are obtained when considering the stratospheric zonal winds from January-February at 15 hPa. Correlations are slightly larger (0.4 for January and 0.38 for February) when restricting the analysis to the period after 1979, but slightly less significant. Westerlies (i.e. eastward, hereafter "west phase") correspond to increased rainfall for the following ISM, compared to easterlies. The significant and systematic propagation of positive correlations across different levels is consistent with the downward phase propagation of the QBO (Baldwin et al., 2001). In addition, at 15 hPa, correlation coefficients are larger when considering only the late IMR and their significance also increases with a confidence level of 99% from January to April before the ISM onset.

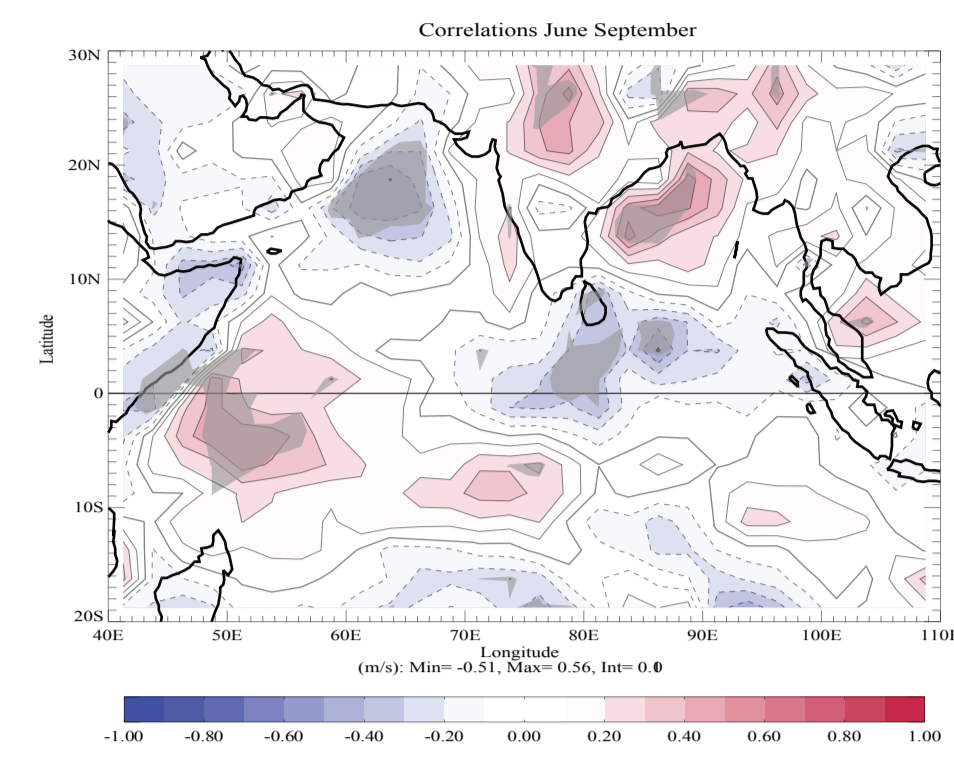


Figure 3. Distribution of correlation coefficients of June-September CMAP precipitation versus equatorial zonal winds at 15 hPa in January-February. Correlation coefficients have been computed for the 1979-2000 period. Correlation coefficients above the 90% confidence level.

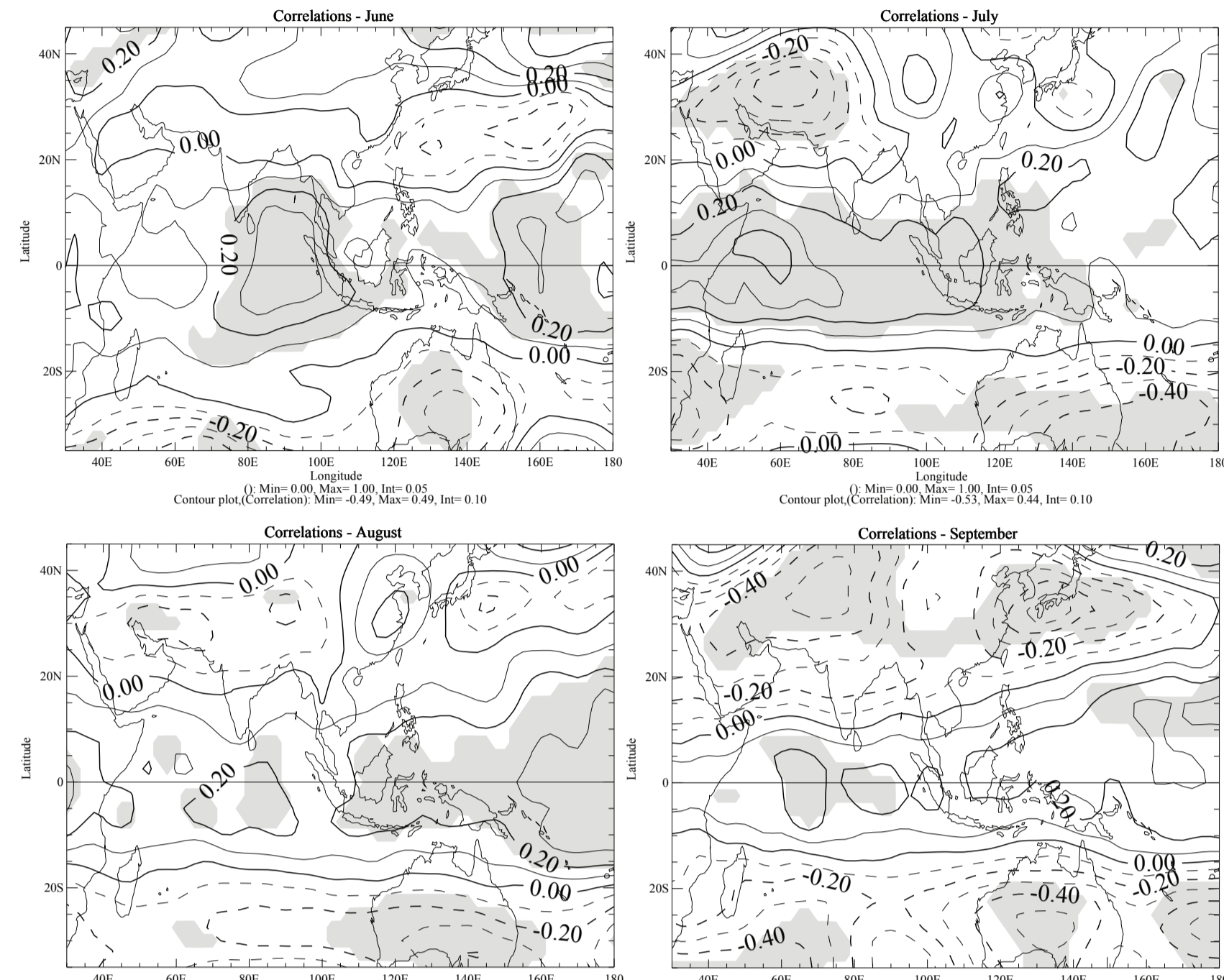


Figure 5. Distribution of monthly correlation coefficients of NCEP tropopause temperature versus equatorial zonal winds at 15 hPa in January-February (June to September). Areas with correlation coefficients above the 90% confidence level are shaded.

VI. 11-year solar cycle / Monsoon

Figure 6 shows correlations between F10.7 and CMAP rainfall fields during the monsoon season. In August and to some extent in July, for higher solar activity, precipitation is reduced over the equatorial Indian Ocean and increased over the western Pacific Ocean and to a lesser extent over part of the Indian subcontinent. Concerning more specifically the Indian subcontinent, while larger precipitation is generally found along the west coast and south of about 20°N for higher solar activity, to the north, rainfall is rather reduced.

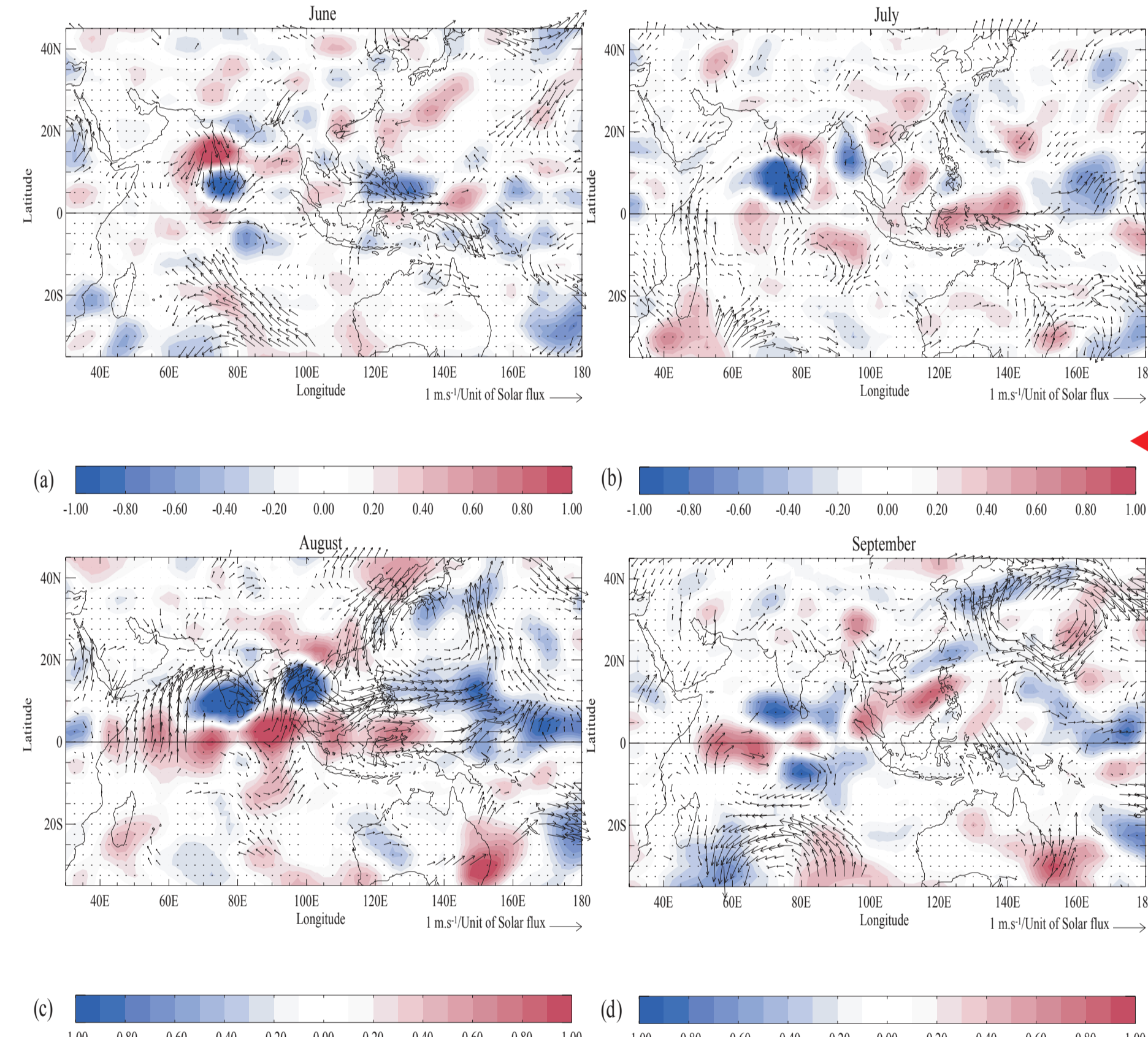


Figure 6. Distribution of correlation coefficients of CMAP precipitation versus F10.7 (June to September). Dotted line contours denote the 90% confidence level.

Figure 7 shows correlations between F10.7 and NCEP-R2 reanalysed stratospheric temperature fields have been determined (Figure 8 for 50 hPa). The signature consists in two lobes of warmer temperatures situated about $25-30^\circ$ from the equator, that peak in July-August (Figure 8b-c) for larger values of F10.7 (significant at 99%). This warming is consistent with a reduction of the convective activity in the equatorial region and an enhancement of convective activity in off-equatorial regions (Kodera, 2004), which is synonymous of a strengthening of the monsoon. However this north/south seesaw in convective activity alone cannot lead to the complex picture presented in Figure 6, and in particular, the opposition equatorial Indian Ocean - warm pool / equatorial western Pacific Ocean observed in August (Figure 6c). Therefore, other explanations have to be found.

Because the variability of the monsoon system is associated to the inter-hemispheric pressure gradient, correlations between the 11-yr solar cycle and the mean sea level pressure have been determined (Figure 9). In June (Figure 9a), a salient feature concerns the large significant positive correlation between the sunspot number and mslp over the Tibetan Plateau and Central Asia. The northwestward shift of the Mascarene High (with significant positive correlations to the west of the subtropical Indian Ocean) could explain the lack of precipitation over the northwest Arabian Sea. Conversely, over the Indian subcontinent, there is a southwest-northeast anomaly gradient in the mslp correlation fields (though correlations are not significant at the 90% level over Peninsular India). This suggests a latitudinal shift of the main axis of the monsoon trough. A more southerly (northerly) position of the monsoon trough is associated with positive (negative) rainfall anomalies over Peninsular India and negative (positive) anomalies over the northeastern part of India (Figure 6). Positive correlations are still present in the western part of the Indian Ocean in July-August, but not any more in September (Figure 9d). There is a high degree of consistency with the response to the solar activity for a period as long as 1871-2001 (not shown).

Correlation and regression patterns between winter F10.7 and detrended SST have been determined (not shown) and indicate a significant cooling of the surface over the southern Indian Ocean and the western Pacific during the pre-monsoon (February-March) period for higher solar activity. These negative SST anomalies before the monsoon in the southern subtropical Indian Ocean, especially in its eastern part, have been shown to be associated with a weaker ISM, especially in August-September (Terray et al., 2003).

VII. Concluding remarks

1. **a west QBO phase (westerlies) may alter deep convective activity along the equator, and, conversely, enhance convection over India.** This brings higher precipitation over the subcontinent compared to an east QBO phase. These results are important to the predictability of ISM rainfall, particularly during the late ISM, since they suggest that the dominant mode of ISM during August and September is partly forced by the phase of the QBO.

2. **In August and to some extent in July, for higher solar activity, precipitation is reduced over the equatorial Indian Ocean and increased over the western Pacific Ocean and over part of the Indian subcontinent.** This results from a combination of effects: on one side, an effect which maximizes in July-August with warmer temperatures in the lower stratosphere for maximum solar activity, and is consistent with a reduction of the convective activity in the equatorial region and an enhancement in off-equatorial regions; on the other side, a modulation of the mean sea level pressure fields, with a more southerly position of the monsoon trough in June, and a northwestward shift of the Mascarene High in July-August associated with a stronger monsoon circulation. High solar activity could also cool the February-March SST in the southern Indian Ocean, which weakens the subsequent monsoon. Observations over the period 1871-2001 confirm these associations. As a result of the reported mechanisms, the 11-year solar cycle has poor skill for foreshadowing the ISM as a whole. However, the associations, occurring on the time scale of months, provide a new insight and would be of considerable interest for further modeling studies.

	JAN	FEB	MAR	APRIL	MAY	JUNE	JULY	AUG
10	0.367*	0.333*						
15	0.400**	0.369*	0.340*	0.303				
20	0.314	0.307	0.334*	0.333**				
30	0.293*	0.266*	0.282*	0.296*	0.266*			
40					0.244	0.343*	0.284**	0.251*
						0.299*	0.318	0.280
							0.257	0.277*

Table 1. Correlation coefficients for the first 8 months of the year between zonal monthly winds at different stratospheric levels, and the IMR during boreal summer (June until September, 1956-2001). Only 90% and more significant values are reported. The symbol * (***) denotes a significance larger than 95% (99%). Values in italics correspond to the correlation coefficients between zonal winds and August-September rainfall.

A west phase of QBO at 15 hPa in January-February is associated in June with a decrease of the surface circulation and, in particular, a weaker Somali Jet, which suggests a delayed ISM onset (Figure 4a). Conversely, in September, the monsoon surface circulation is significantly reinforced during the west phase of the QBO, which means a positive precipitation anomaly over central India and a deepening of the monsoon trough (Figure 4d). Anomalous and significant circulation patterns are also observed in the southern Indian Ocean during the late ISM: the Mascarene High is stronger and shifted westward during the west phase of the QBO, which is consistent with a stronger monsoon (Terray et al., 2003).

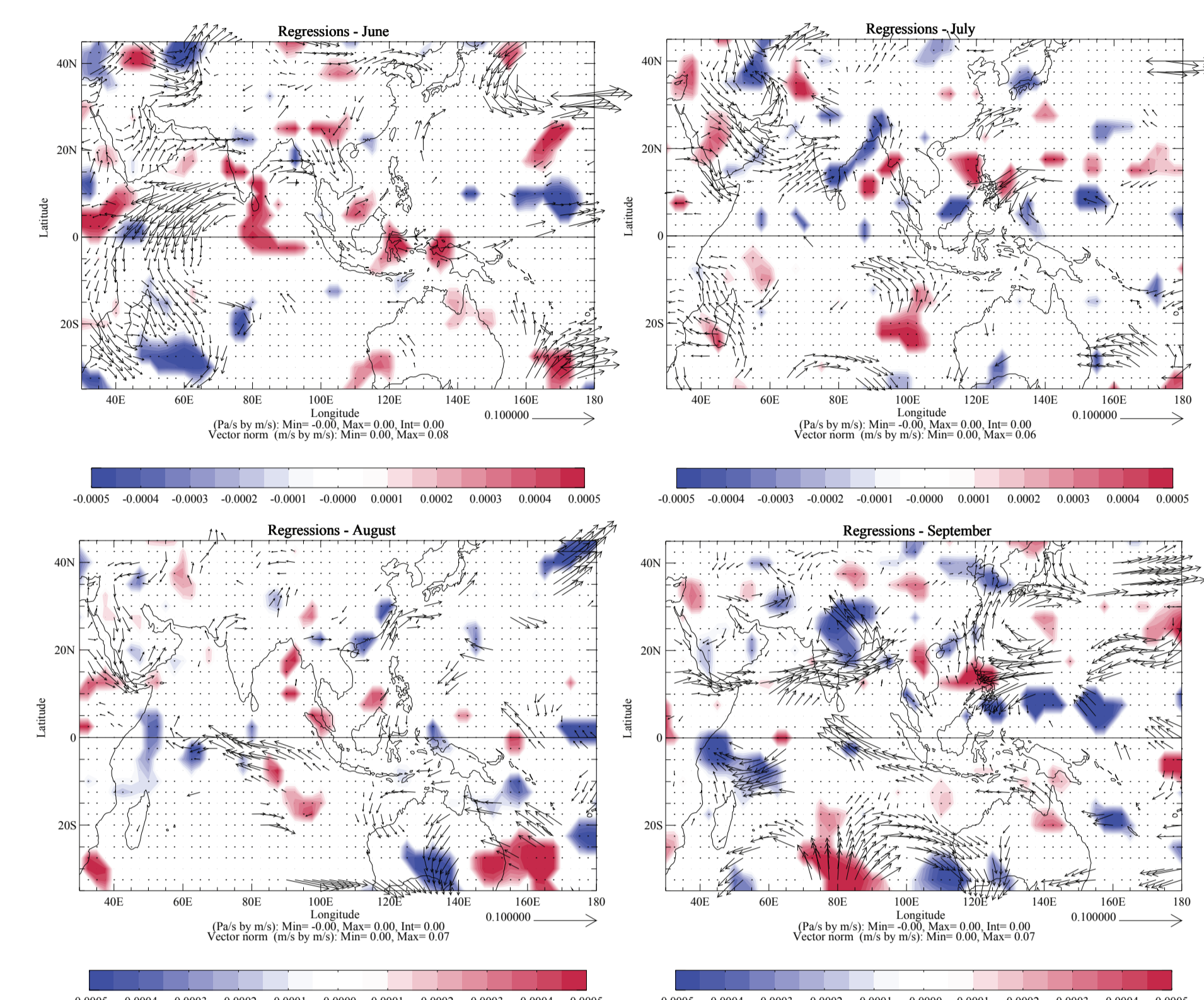


Figure 4. Distribution of monthly regression coefficients of NCEP-R2 850 hPa wind and 500 hPa vertical velocity versus equatorial zonal winds at 15 hPa in January-February (June to September). Maps only show wind vectors and omega values corresponding to regression coefficients above the 90% confidence level.

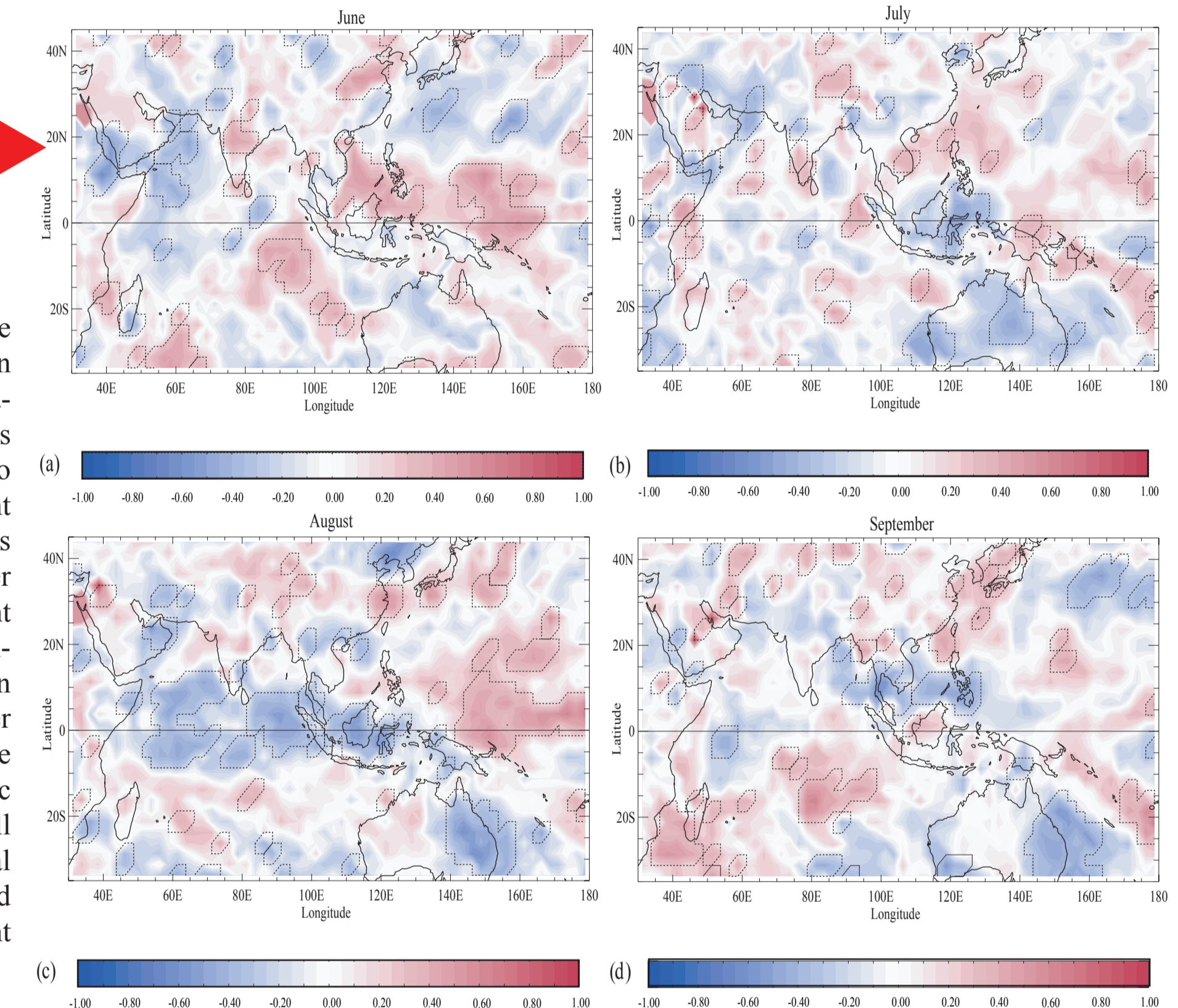


Figure 7. Distribution of monthly regression coefficients of 850 hPa wind and correlation coefficients of 500 hPa vertical velocity versus F10.7 (June to September). Maps only show wind vectors and omega values corresponding to coefficients above the 90% confidence level.

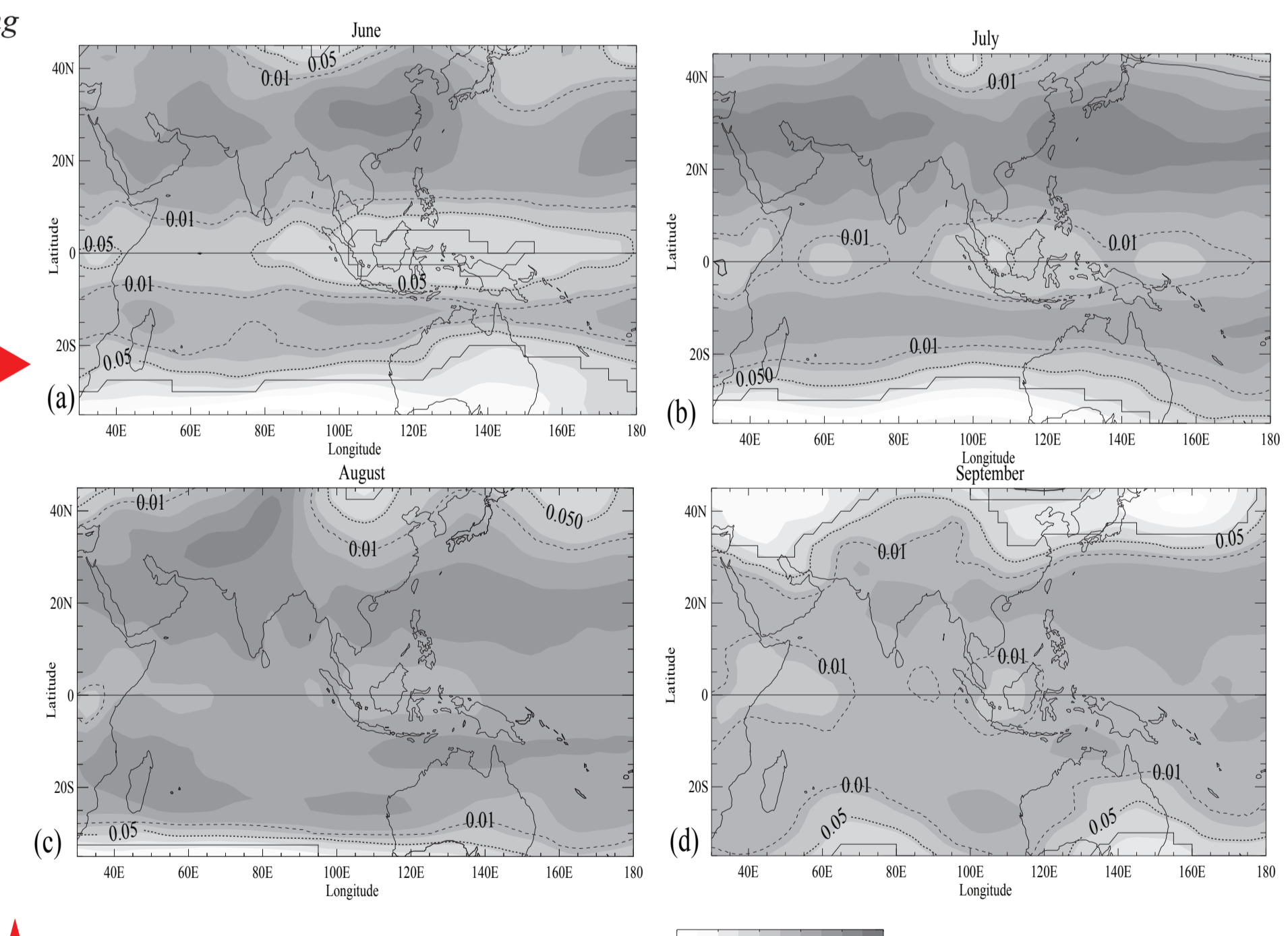


Figure 8. Distribution of correlation coefficients of 50 hPa temperature versus F10.7 (June to September). The confidence level has been superimposed (dashed line: 90%, dotted line: 95% and continuous line: 99%).

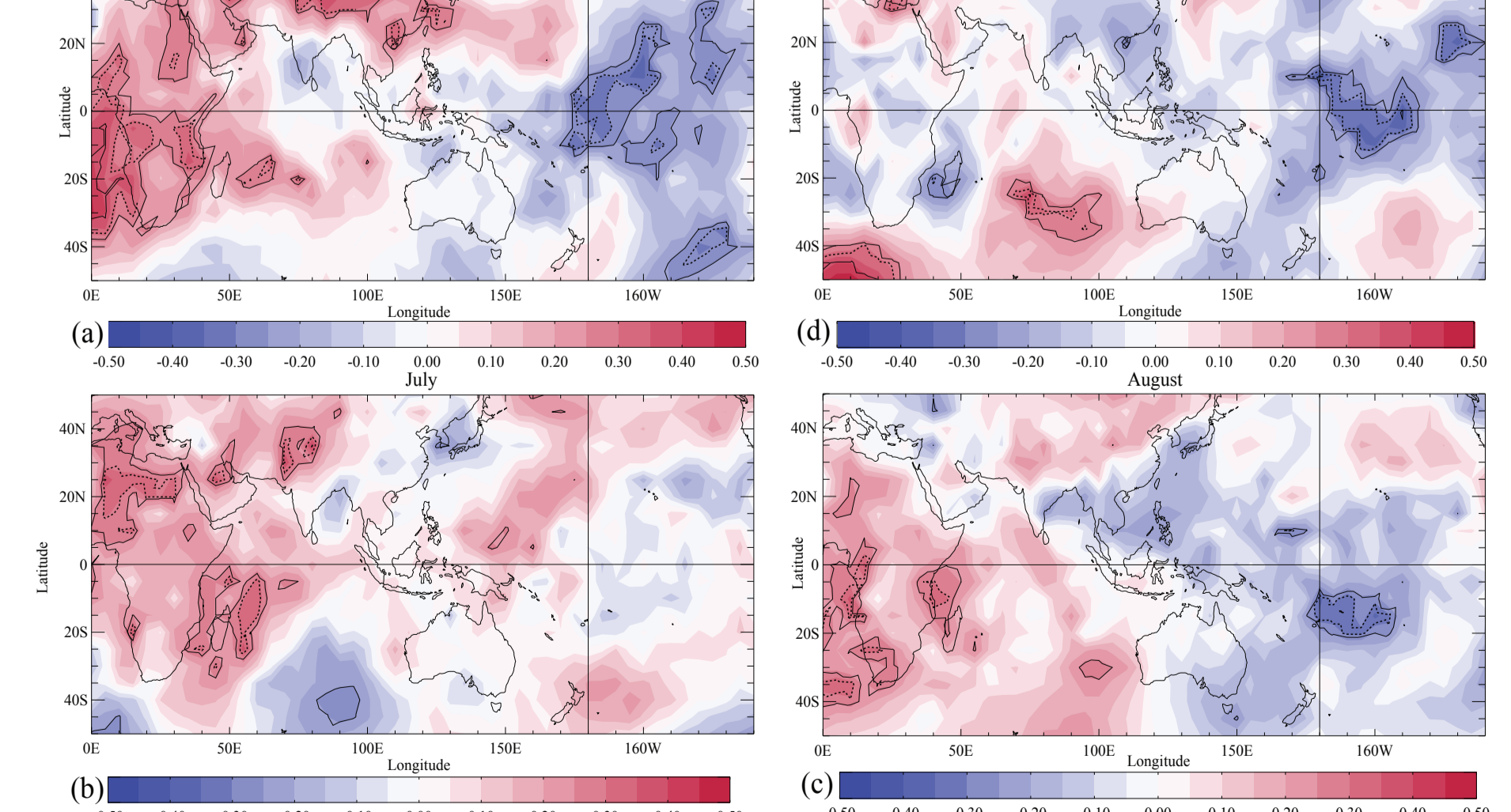


Figure 9. Distribution of monthly correlation coefficients of mslp versus the sunspot value (June to September). Continuous (dotted) line contours denote the 90% (95%) confidence level. Note that the scale is from -0.5 to 0.5.